ELSEVIER

Journal of Alloys and Compounds 311 (2000) 292–298

Journal of ALLOYS AND COMPOUNDS

www.elsevier.com/locate/jallcom

Improved temperature and corrosion behaviour of nanocomposite $Nd_2(Fe,Co,M)_{14}B/\alpha$-Fe magnets

M. Jurczyk*, J. Jakubowicz

Institute of Materials Science and Engineering, Poznañ University of Technology, M. Sklodowska-Curie 5 Sq., 60-965 Poznañ, Poland

Received 4 June 2000; accepted 26 June 2000

Abstract

The characteristics of the magnetic properties nanocomposite $Nd_2(Fe,Co,M)_{14}B/\alpha$-Fe magnets obtained by high energy ball milling and powder metallurgy routes have been improved by appropriate Al–Cr, Cr, Zr additions. Using a single phase close to the stoichiometric composition, nanocomposite $Nd_{12.6}(Fe,Co,M)_{81.4}B_6/\alpha$-Fe magnets with better temperature stability are produced, due to the disappearance of the Nd-rich grain boundary phase in $Nd_2(Fe,Co)_{14}B/\alpha$-Fe materials. If the content of the soft magnetic α-Fe phase in $Nd_2(Fe,Co,M)_{14}B/\alpha$-Fe composities increases, the thermal stability of the coercivity increases, too. For a $Nd_{12.6}Fe_{69.3}Co_{11.6}Zr_{0.5}B_6/\alpha$-Fe magnet, containing 37.5 vol% α-Fe, the temperature coefficients (from 293 to 413 K) of remanence $\alpha(J_r)$ and coercivity $\beta(_JH_c)$ are: -0.07 and -0.35% K^{-1}, respectively. Nanocomposite magnets appears to be more corrosion resistant than sintered Nd–Fe–B magnets.

Keywords: Rare earth compounds; Transition metal compounds; Permanent magnets; Nanostructures; Powder metallurgy

1. Introduction

In the absence of intercrystalline exchange coupling, the remanent magnetic polarization J_r of an isotropic magnetic material consisting of a random array of magnetic particles, exhibiting uniaxial magnetocrystalline anisotropy, should equal one half of the saturation magnetic polarization J_s, i.e. the reduced remanent magnetic polarization $\alpha = J_r/J_s = 0.5$ (Stoner–Wohlfarth theory [1]). Recent studies have reported significantly higher values of J_r, and hence values of larger than 0.5, in nanocomposite two-phase mixtures consisting of magnetically hard and soft phases [2–8]. Remanence enhancement has been reported in a variety of nanostructured Fe-rich rare earth magnet alloys, prepared by recrystallization either of melt-spun [4] or of mechanically alloyed materials [5,9]. There are two types of remanence enhanced materials: (i) those composed of two phases ($Nd_2Fe_{14}B$ and α-Fe) with relatively low boron content and (ii) those composed of three phases ($Nd_2Fe_{14}B$, Fe_3B and α-Fe) with high boron content. The development of high remanent magnetic polarization and a technologically useful intrinsic coercivity requires the formation of an optimum microstructure consisting of a nanocomposite two-phase mixture of magnetically hard ($Nd_2Fe_{14}B$) and soft (α-Fe or Fe_3B and α-Fe) phases, with mean grain sizes below 30 and below 15 nm located on the grain boundaries, respectively. The ultra fine soft magnetic grains, of high saturation magnetic polarization, enhance the low remanent magnetic polarization of the hard phase by a form of exchange coupling [10].

The relationship between the microstructure and the magnetic properties of nanocrystalline two-phase magnets has been explored, using micromagnetic calculations, by Kneller and Hawig [11], Skomski [12] and Schrefl et al. [13]. Micromagnetic calculations by Schrefl et al. [14] on cellular structures in two and three dimensions have shown that the size of the soft grains should ideally be about twice the domain wall width (δ_w) of the hard magnetic phase. The coercivity mechanism in two-phase magnetic materials, RE-3*d*/3*d*-type, has been described by Kneller and Hawig, too [11]. These authors have investigated the combined effect of two suitably dispersed and mutually exchange-coupled phases. The first of these phases is magnetically hard (large uniaxial anisotropy constant K) and provides a high coercivity. The second phase is magnetically soft but has a larger magnetic ordering temperature. It is the comparatively high saturation magnetic polarization (J_s) of the soft phase which provides a high remanent magnetic polarization. According to this

*Corresponding author. Fax: +48-61-665-3576.
E-mail address: jurczyk@sol.put.poznan.pl (M. Jurczyk).

0925-8388/00/$ – see front matter
PII: S0925-8388(00)01114-2

model, the soft phase is acted upon by two fields, one due to the externally applied field and the other due to the neighbouring hard phase. The field due to the hard magnetic phase tries to prevent the reversal of the soft magnetic moments upon reversal of the externally applied field. As a result, the intrinsic coercivity drops rapidly when either the soft phase grain size is large or its volume fraction increases [15].

Magnetic materials with enhanced remanent magnetic polarization were first reported in a single-phase system by McCallum et al. [3] for melt-spun Nd–Fe–B alloys containing Si or Al. Coehoorn et al. [4] described a new type of Nd-poor $Nd_{3.8}Fe_{77}B_{19.2}$ ribbons, where the hard phase is $Nd_2Fe_{14}B$ and the soft phase is mainly Fe_3B. Similarly, remanent magnetic polarization enhancements has been reported in a variety of nanostructured Fe-rich rare-earth magnet alloys, prepared by recrystallization of either mechanically alloyed [9,5], or high-energy ball-milled materials [2]. Considerable higher rare earth concentrations were used by Manaf et al. [16]. These authors prepared nanocrystalline exchange coupled alloys from melt-spun $Nd_9Fe_{85}B_6$, where the α-Fe soft phase is exchange coupled to the hard magnetic $Nd_2Fe_{14}B$ phase. A better temperature stability of the intrinsic coercivity but lower remanent magnetic polarizations were reported for optimally annealed melt-spun alloys of the $Nd_9(Fe,Co)_{85}B_6$-type [17].

Also, mechanical alloying was used to produce two-phase nanocrystalline alloys. Gong et al. [5] investigated two-phase nanocomposite magnets in which the minor $Nd_2Fe_{14}B$ hard phase is coupled to an α-Fe or $Fe_{70}Co_{30}$ soft phase. Jurczyk [2,7] used alloys of much lower rare earth content. After mechanical alloying $Nd_2(Fe,Co)_{14}B$ with α-Fe powder and annealing, the volume fraction of the magnetically soft α-Fe phase was 40% with grain sizes of about 11 nm. Addition of Zr has been shown to be advantageous in improving the energy product and squareness of the hysteresis loop in two-phase nanocomposite $(Nd,Dy)_2(Fe,Co,Zr)_{14}B/\alpha$-Fe materials [2]. Exchange coupled nanocrystalline $Nd_2Fe_{14}B/\alpha$-Fe alloys with large volume fractions of α-Fe and large remanence enhancements were reported also by Wecker et al. [18] and Miao et al. [19].

As was mentioned above, the remanence enhanced $Nd_2Fe_{14}B/\alpha$-Fe-type materials are composed of the following phases: $Nd_2Fe_{14}B$ (magnetically hard phase) and α-Fe or Fe_3B and α-Fe (magnetically soft phases). It is well known that the main problems of the $Nd_2Fe_{14}B$ phase are (i) their low Curie temperature and (ii) their low corrosion resistance, particularly for wet corrosion. This is because the Nd-rich intergranular phase, under humidity and temperature, transforms into Nd hydrides, which are very brittle, inducing the non-oxidized grains of the main phase to be released from the magnet [20,21]. Therefore, much effort has been spent, till now, to overcome these problems. The substitution of cobalt for iron has been tried because Co improves the Curie temperature by increasing the 3*d*–3*d* exchange interaction. But, unfortunately, it also induces large coercivity losses due to modifications in the Nd-rich phase microstructure, e.g. precipitation of $Nd(Co,Fe)_2$ [22]. Present-day sintered Nd–Fe–B magnets contain a limited amount of Co, mainly in order to increase the stability against corrosion. The use of addition elements such as Co or Zr slows down the corrosion process by forming corrosion resistant intergranular Nd–Co [23–26] or Fe–Zr [27] phases. With increasing amount of Co one observes stronger brake acid corrosion [28]. According to Fidler [29] there are two types of dopant elements: type M_x (Al,Cu,Ga,Sn,Ge,Zn) and type M_y (V,Mo,W,Nb,Ti,Zr). Type M_x dopants form Nd–M_x or Nd–Fe–M_x intergranular phases. Type M_y dopants form M_y–B or Fe–M_y–B intergranular and intragranular phases. Because they are corrosion-resistant (with higher corrosion potentials), the phases which are formed at the grain boundaries obstruct the oxidation of the Nd-rich regions. On the other hand, the precipitates formed inside the $Nd_2Fe_{14}B$ grains could be responsible for the slowing down of the corrosion process inside the grains [30]. A Cr additive of at least 1 at% is very effective in corrosion protection [31]. Cr and Co additives lead to increase the tendency to passivation [32]. As no Nd-rich phase is formed in a $Nd_{12.6}(Fe,Co,M)_{81.4}B_6/\alpha$-Fe nanocomposite, this material should be more corrosion-resistant than a Nd–Fe–B sintered magnet.

The aim of this work is to investigate the role of the dopants elements, such as Al–Cr, Cr, Zr in improving the thermal stability and corrosion resistance of $Nd_2(Fe,Co,M)_{14}B/\alpha$-Fe-type magnets. Using a single phase of near stoichiometric composition, nanocomposite $Nd_{12.6}(Fe,Co,M)_{81.4}B_6/\alpha$-Fe magnets were produced with different contents of the soft magnetic α-Fe phase.

2. Experimental details

Two phase nanocomposite $Nd_{12.6}(Fe,Co,M)_{81.4}B_6/\alpha$-Fe materials (M = Al–Cr, Cr, Zr) were prepared by high-energy ball-milling (HEBM) of $Nd_2(Fe,Co,M)_{14}B$-type powder (with an average size less than 90 μm) and 0, 10 or 37.5 vol% of α-Fe powder (with particle size less than 10 μm) in an SPEX 8000 mixer mill. The as-milled powder was then heat-treated at 870–1120 K for 30 min in order to crystallize the tetragonal $Nd_2Fe_{14}B$-type phase [7].

The powders were examined by XRD analysis at the various stages during milling, prior to annealing and after annealing. Typical crystallite sizes were estimated from the half-width of lines using the Scherrer equation [33] given by:

$$D_{hkl} = k\lambda/\beta \cos \Theta \quad (1)$$

where D_{hkl} is the crystallite size estimated from a (*hkl*)

line, k the Scherrer constant, β the half-width, λ the X-ray wavelength and Θ the diffraction angle.

The phases were identified by XRD as well as by scanning electron microscopy (SEM) with an energy-dispersive X-ray microanalysis system (EDS). The SEM technique was used to follow the changes in size and shape of the HEBM processed Nd–Fe–B-type powders.

Magnets were produced by one of two methods. Spherically shaped samples ($\phi = 5$ mm), for measurements of the magnetic properties at room temperature, were made by mixing the powders with epoxy resin in suitable moulds in an applied magnetic field of 2.1 MA m^{-1}. The filling fraction was 0.8 and all data have been normalized with respect to 100% density. For the measurements of magnetic properties at higher temperatures as well as for corrosion tests, full density magnets were produced by hot pressing. In the series of experiments reported here, the temperatures of hot pressing were varied over the range 970–1130 K and the pressing times from 5 s to 2 min. Cylindrical magnets with a diameter of 5 mm and a height of about 3 mm were produced. Experimental densities of the magnets were determined by weighing under cyclohexane.

Magnetic characteristics were measured by one of two methods: VSM or hysteresis graph. On selected samples, with and without the addition of Co, the Curie temperatures were determined using a thermogravimetric method (TGA), modified by the addition of two small permanent magnets to operate as a low-field Faraday balance. The samples for TGA measurements were in the form of loose powder, sealed under an argon atmosphere in a quartz capillary tube and pre-magnetized before measurement. T_c were determined from these measurements by plotting J^2 vs. T and extrapolating to $J = 0$.

The demagnetization curves of magnets are temperature-dependent. This dependence is characterized by the temperature coefficients of the remanent magnetic polarization, $\alpha(J_r)$ and the intrinsic coercivity, $\beta({}_JH_c)$. The corrosion resistance test on the nanocrystalline $Nd_2(Fe,Co,M)_{14}B/\alpha$-Fe-type magnets was carried out by corrosion potential measurement (3% NaCl water solution and 50 mV min^{-1} scanning speed).

3. Results and discussion

For all samples, XRD analysis showed that after 48 h high energy ball milling the alloy had decomposed into an amorphous phase and nanocrystalline α-Fe (Fig. 1a). Using $Nd_{12.6}Fe_{67.8}Co_{11.6}Cr_2B_6/\alpha$-Fe with a 37.5% volume fraction of magnetically soft α-Fe phase as a representative alloy example, the behaviour of the grain size and the formation of the hard and soft phases can be tracked through the anneal. At the conclusion of milling the mean grain size of the crystalline component was of order 12 nm

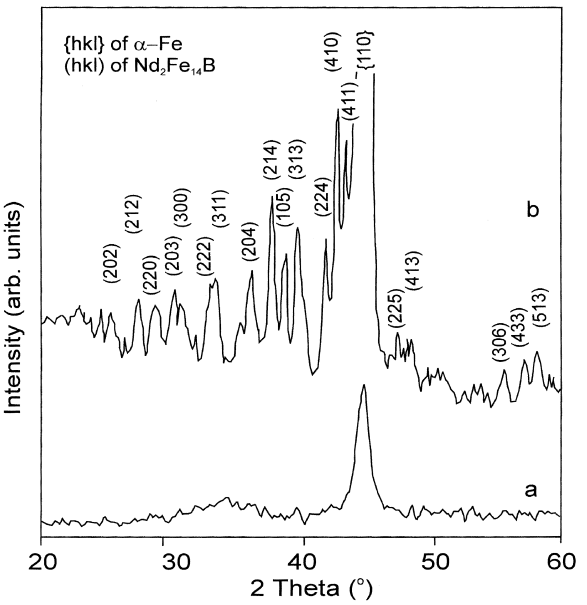

Fig. 1. XRD spectra for the $Nd_{12.6}Fe_{67.8}Co_{11.6}Cr_2B_6/\alpha$-Fe with a 37.5% volume fraction of magnetically soft α-Fe phase: (a) HEBM for 48 h, (b) heat-treated at 950 K for 30 min (Cu Kα).

and after annealing in high purity argon at 950 K for 30 min it had increased to about 37 nm. Annealing the powder results in the formation of the tetragonal $Nd_2Fe_{14}B$-type crystal structure (Fig. 1b) which coexists with the α-Fe phase, resulting in a two-phase nanocomposite material.

All the powders prepared by the HEBM process are magnetically isotropic and the intrinsic magnetic properties of studied materials are given in Table 1. The intrinsic coercivity ${}_JH_c$, and the reduced remanent magnetic polarization α, of $Nd_{12.6}Fe_{66.8}Co_{11.6}Al_1Cr_2B_6/\alpha$-Fe powder with a volume fraction of magnetically soft α-Fe phase of 10%, as a function of annealing temperature for 30 min anneal, are shown in Fig. 2. A maximum intrinsic coercivity of 638 kA m^{-1} is obtained at an annealing temperature of 970 K. ${}_JH_c$ is lower in powders annealed at both lower and higher temperatures, as the grain size of the soft α-Fe phase is either too small or too large for optimum exchange coupling [11]. The reduced remanent magnetic polarization decreases from 0.78 to 0.66 as the annealing temperature increases. Generally the grain growth which occurs at the higher temperatures leads to deterioration in magnetic properties. The principal advantages of Co addition to $Nd_2Fe_{14}B/\alpha$-Fe are increases in the Curie temperature of the hard phase, and a possible increase in the saturation polarization, arising from the higher saturation of Fe(Co), compared to that of pure α-Fe [2]. Additionally, the Curie temperature increases with increasing excess iron content in $Nd_{12.6}Fe_{69.8}Co_{11.6}B_6/\alpha$-Fe, resulting in a ~20 K enhancement over the Curie temperature of the pure $Nd_2Fe_{14}B$ phase with 37.5 vol% excess of α-Fe.

The magnetic properties of the powders processed by

Table 1
Magnetic properties of $Nd_2Fe_{14}B/\alpha$-Fe-type compounds after HEBM and optimal heat treatment

Material composition	α-Fe content (vol%)	J_s (T)	J_r (T)	α (J_r/J_s)	${}_JH_c$ (kA m^{-1})
$Nd_{12.6}Fe_{69.8}Co_{11.6}B_6/\alpha$-Fe	0	1.15	0.51	0.44	420
	10	1.19	0.50	0.42	322
	37.5	1.62	0.55	0.34	208
$Nd_{12.6}Fe_{69.3}Co_{11.6}Zr_{0.5}B_6/\alpha$-Fe	0	0.96	0.67	0.70	680
	10	1.16	0.86	0.74	662
	37.5	1.62	1.14	0.70	504
$Nd_{12.6}Fe_{68.8}Co_{11.6}Cr_1B_6/\alpha$-Fe	37.5	1.60	1.14	0.71	540
$Nd_{12.6}Fe_{67.8}Co_{11.6}Cr_2B_6/\alpha$-Fe	0	0.99	0.62	0.63	825
	10	1.12	0.81	0.72	840
	37.5	1.55	1.10	0.71	760
$Nd_{12.6}Fe_{65.8}Co_{11.6}Cr_4B_6/\alpha$-Fe	37.5	1.26	0.88	0.70	740
$Nd_{12.6}Fe_{66.8}Co_{11.6}Al_1Cr_2B_6/\alpha$-Fe	0	1.09	0.56	0.51	825
	10	1.11	0.85	0.76	638
	37.5	1.50	1.08	0.72	586

HEBM method depends on the composition of the starting material. Fig. 3 shows the dependence of remanent magnetic polarization and intrinsic coercivity of $Nd_{12.6}Fe_{69.8-x}Co_{11.6}Cr_xB_6/\alpha$-Fe with a 37.5% volume fraction of magnetically soft phase as a function of the Cr concentration. Increasing Cr content leads initially to an increase in remanent magnetic polarization, giving a maximum at $x=1$, while for $x>1$, J_r decrease considerably. Note that for $Nd_{12.6}Fe_{69.8}Co_{11.6}B_6/\alpha$-Fe as well as $Nd_{12.6}Fe_{81.4}B_6/\alpha$-Fe with 37.5% of α-Fe, the reduced remanent magnetic polarization α differs from the expected value of approximately 0.5 in samples with a low intrinsic coercivity due to demagnetization effects. The intrinsic coercivity initially increased for $x=2$ and then decreased for higher concentrations. An initial substitution of Co results in an increase in ${}_JH_c$ from 160 to 208 kA m^{-1}; the subsequent addition of Cr causes a further increase in ${}_JH_c$ from 208 kA m^{-1} ($x=0$) to 760 kA m^{-1} ($x=2$). The improvement in the intrinsic coercivity by the addition of Cr could be attributed to an increase in the anisotropy field [34,35]. Alternatively, Cr may play a role in grain refinement. Alloys $Nd_{12.6}Fe_{81.4}B_6/\alpha$-Fe containing Cr and Co with 37.5% of α-Fe by volume exhibit most desirable magnetic properties, having J_r of order of 1.1 T, ${}_JH_c$ in excess of 760 kA m^{-1} and a reduced remanent magnetic polarization α of about 0.7.

Fig. 4A, shows demagnetization curves of the $Nd_{12.6}Fe_{69.8}Co_{11.6}B_6/\alpha$-Fe, $Nd_{12.6}Fe_{67.8}Co_{11.6}Cr_2B_6/\alpha$-Fe

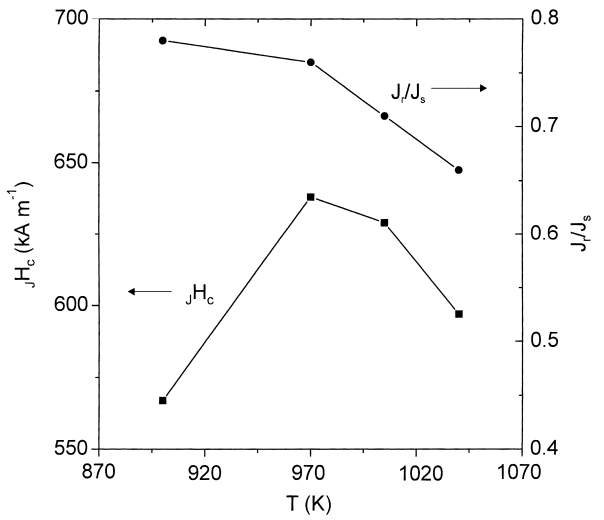

Fig. 2. The intrinsic coercivity ${}_JH_c$, and the reduced remanent magnetic polarization α of $Nd_{12.6}Fe_{66.8}Co_{11.6}Al_1Cr_2B_6/\alpha$-Fe powder with a volume fraction of magnetically soft α-Fe phase of 10%, as a function of annealing temperature for 30-min anneal.

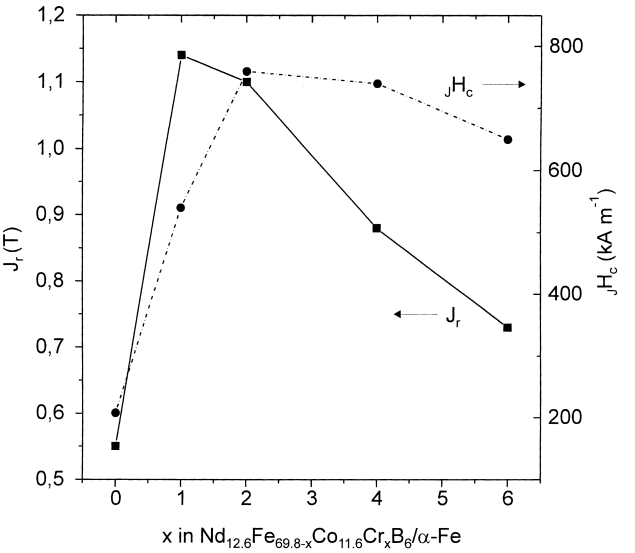

Fig. 3. Dependence of remanent magnetic polarization and intrinsic coercivity of $Nd_{12.6}Fe_{69.8-x}Co_{11.6}Cr_xB_6/\alpha$-Fe with a 37.5% volume fraction of magnetically soft phase as a function of the Cr concentration.

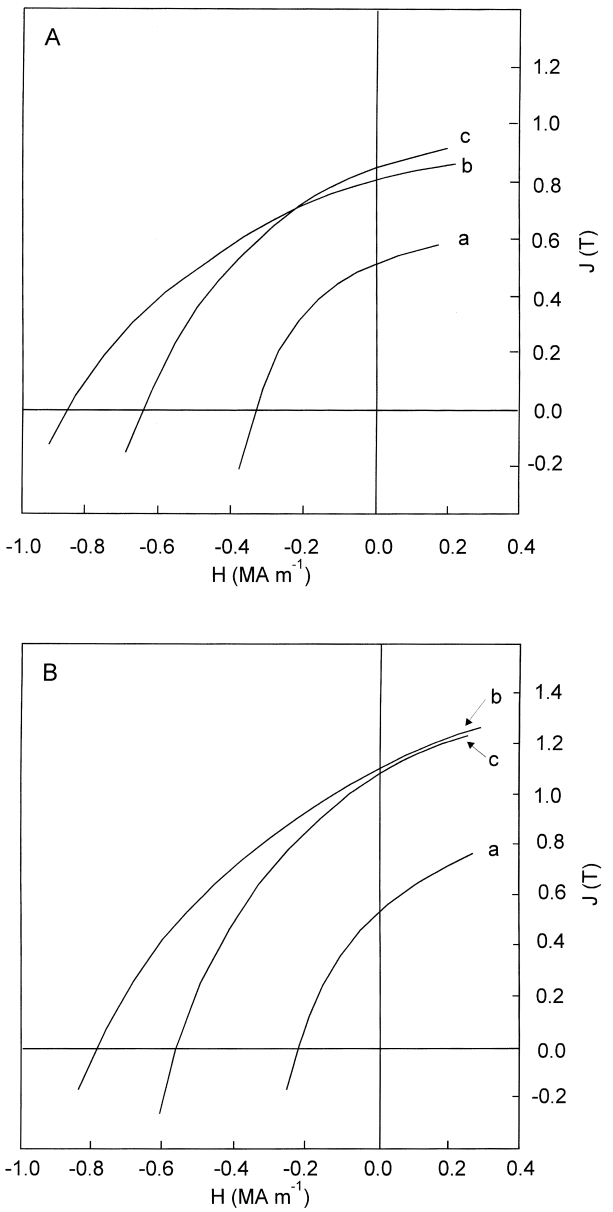

Fig. 4. Demagnetization curves of (a) $Nd_{12.6}Fe_{69.8}Co_{11.6}B_6$/α-Fe, (b) $Nd_{12.6}Fe_{67.8}Co_{11.6}Cr_2B_6$/α-Fe and (c) $Nd_{12.6}Fe_{66.8}Co_{11.6}Al_1Cr_2B_6$/α-Fe powders, with a volume fraction of α-Fe of 10% (A) and 37.5% (B) after HEBM and optimal annealing treatment (all data have been normalized with respect to 100% density).

and $Nd_{12.6}Fe_{66.8}Co_{11.6}Al_1Cr_2B_6$/α-Fe powders, with a volume fraction of α-Fe of 10% after HEBM and optimal annealing treatment. The Cr- and AlCr-free $Nd_{12.6}Fe_{69.8}Co_{11.6}B_6$/α-Fe powder has a lower remanent magnetic polarization and a lower intrinsic coercivity. When a small amount of Cr, Al–Cr and other metal, such as Zr, is added to the Co-substituted $Nd_{12.6}Fe_{69.8}Co_{11.6}B_6$/α-Fe, J_r and $_JH_c$ are significantly improved (see Table 1). Bonded magnets of J_r and $_JH_c$ ranging from 0.81 T and 840 kA m^{-1} to 1.1 T and 760 kA m^{-1} have been produced from $Nd_{12.6}Fe_{67.8}Co_{11.6}Cr_2B_6$/α-Fe, with a 10 and 37.5% volume fraction of soft α-Fe phase, respectively. Fig. 4B, shows demagnetization curves of the $Nd_{12.6}Fe_{69.8}Co_{11.6}B_6$/α-Fe, $Nd_{12.6}Fe_{67.8}Co_{11.6}Cr_2B_6$/α-Fe and $Nd_{12.6}Fe_{66.8}Co_{11.6}Al_1Cr_2B_6$/α-Fe powders with 37.5% α-Fe. The $Nd_{12.6}Fe_{67.8}Co_{11.6}Cr_2B_6$/α-Fe powder showed the highest intrinsic coercivity $_JH_c$ of 760 kA m^{-1}, which compares well with 800 kA m^{-1} reported earlier by Hirosawa et al. [36] for melt-spun and annealed $Nd_{4.5}Fe_{57}Cr_{20}B_{18.5}$ ribbons. Hirosawa et al. [36] note also that powders containing 20% chromium failed to exhibit a remanent magnetic polarization J_r, larger than 0.53 T.

Some HEBM and heat treated $Nd_{12.6}Fe_{69.8-x}Co_{11.6}M_xB_6$/α-Fe-type powders have been compacted by hot pressing to form magnets. A systematic study of the effect of pressing temperature and time on the remanent magnetic polarization, intrinsic coercivity and density, has been carried out. A summary of the magnetic properties of produced magnets are given in Table 2. Full densification (about 97 vol%) in $Nd_2(Fe,Co,M)_{14}B$/α-Fe powders with different volume fractions of magnetically soft α-Fe phase was achieved for $T \geq 1070$ K. Generally, pressing at higher temperatures results in a decrease in $_JH_c$ and an increase in both J_r, and density, ρ (Table 2). It is likely that grain growth is occurring at the higher temperatures, leading to a deterioration in the magnetic properties. Hot pressing at 1070 K of $Nd_{12.6}Fe_{69.3}Co_{11.6}Zr_{0.5}B_6$/α-Fe powders, containing 37.5% volume fraction of magnetically soft α-Fe, produced isotropic magnets with $J_r = 0.99$ T, $_JH_c = 430$ kA m^{-1}, $\rho = 7.59$ g cm^{-3}. It is interesting to note that Hirosawa and Kanekiyo for nanocomposite magnets made from heat treated flakes of $Nd_{5.5}Fe_{66}B_{18.5}Cr_5Co_5$ reported an intrinsic coercivity of about 600 kA m^{-1} [37].

Table 2
Magnetic properties and experimental density, at room temperature, for some nanocrystalline $Nd_2(Fe,Co,M)_{14}B$/α-Fe magnets hot pressed at different temperatures

Composition	Hot pressing temperature (K)	J_r (T)	$_JH_c$ (kA m^{-1})	ρ (g cm^{-3})
$Nd_{12.6}Fe_{69.3}Co_{11.6}Zr_{0.5}B_6$/10 vol% α-Fe	1020	0.83	590	7.05
	1070	0.80	525	7.61
	1130	0.81	460	7.62
$Nd_{12.6}Fe_{69.3}Co_{11.6}Zr_{0.5}B_6$/37.5 vol% α-Fe	1020	1.05	440	7.03
	1070	0.99	430	7.59
	1130	0.76	420	7.65

Table 3
Temperature coefficients of remanent magnetic polarization $\alpha(J_r)$ and intrinsic coercivity $\beta({}_JH_c)$ for nanocomposite $Nd_2(Fe,Co,M)_{14}B/\alpha$-Fe magnets hot pressed at 1020 K with different volume fraction of α-Fe in comparison with Nd–Fe–B sintered magnet

Composition	Content of soft magnetic phase of α-Fe (vol%)	$\alpha(J_r)$ (% K^{-1}) 293÷413 K	$\beta({}_JH_c)$ (% K^{-1}) 293÷413 K
$Nd_{12.6}Fe_{69.3}Co_{11.6}Zr_{0.5}B_6/\alpha$-Fe	10	−0.07	−0.36
$Nd_{12.6}Fe_{69.3}Co_{11.6}Zr_{0.5}B_6/\alpha$-Fe	37.5	−0.07	−0.35
Nd–Fe–B sintered magnet[a]	0	−0.12	−0.63

[a] Data were taken from Ref. [40].

The demagnetization curves are temperature-dependent. This dependence is characterized by the temperature coefficients of the remanent magnetic polarization, $\alpha(J_r)$ and the intrinsic coercivity, $\beta({}_JH_c)$. The temperature coefficients (from 293 to 413 K) of α and β for studied magnets are given in Table 3. These coefficients of $Nd_{12.6}Fe_{69.3}Co_{11.6}Zr_{0.5}B_6/\alpha$-Fe magnet with a content of the soft magnetic phase of 37.5 vol% are −0.07 and −0.35% K^{-1}, respectively. These have to be compared with −0.09 and −0.32% K^{-1} for the $Nd_{5.5}Fe_{66}B_{18.5}Cr_5Co_5$ nanocomposite magnet [36,37]. It is worth noting that partial replacement of Fe by Co, Zr or Al–Cr substantially reduces α and β in the $Nd_{12.6}Fe_{69.8}Co_{11.6}B_6/\alpha$-Fe magnet with a 37.5% volume fraction of α-Fe. Attempts at producing anisotropy by die-upsetting of $Nd_2(Fe,Co,Zr)_{14}B/\alpha$-Fe powders were unsuccessful.

Also, the corrosion resistance of some $Nd_2(Fe,Co,M)_{14}B/\alpha$-Fe magnets has been studied by potentiostatic measurements. $Nd_{12.6}(Fe,Co,M)_{81.4}B_6/\alpha$-Fe-type magnets were expected to have better corrosion resistance. Table 4, reports the corrosion rate for two-phase nanocomposite $Nd_{12.6}(Fe,Co,M)_{81.4}B_6/\alpha$-Fe magnets with a volume content of the soft magnetic phase of 37.5 vol%. The corrosion resistance is improved especially for M= Al_1Cr_2, where the corrosion rate is 0.037 mm $year^{-1}$. Independently, the oxidation process of the nanocomposite $Nd_{12.6}(Fe,Co,Zr)_{81.4}B_6/\alpha$-Fe was investigated at higher temperatures by Mössbauer spectroscopy and was compared to that of the $Nd_2Fe_{14}B$ phase [38,39]. It appears that oxidation of several nanocomposite magnets is slower in comparison to that of the $Nd_2Fe_{14}B$ phase in Nd–Fe–B sintered magnets. The microstructural investigations revealed that the annealed powders are composed of almost spherical aggregates of $Nd_2(Fe,Co,Zr)_{14}B/\alpha$-Fe and α-Fe(Co) nanograins. The slowing of the dissociation process suggested that in the aggregates the α-Fe(Co) phase acts as a protective layer for the $Nd_2(Fe,Co,M)_{14}B$ nanograins against the oxidation [38]. Thus, a nanocomposite powder appears to be intrinsically more corrosion resistant than a sintered Nd–Fe–B magnet [39].

Table 4
The values of corrosion speed for some of studied $Nd_2(Fe,Co,M)_{14}B/\alpha$-Fe magnets (37.5 vol% of α-Fe)

Sample	Soft magnetic phase α-Fe (vol%)	Corrosion (mm $year^{-1}$)
$Nd_{12.6}Fe_{66.8}Co_{11.6}Al_1Cr_2B_6/\alpha$-Fe	37.5	0.037
$Nd_{12.6}Fe_{69.3}Co_{11.6}Zr_{0.5}B_6/\alpha$-Fe	37.5	0.107

4. Conclusions

A range of remanence enhanced $Nd_{12.6}Fe_{69.8-x}Co_{11.6}M_xB_6/\alpha$-Fe (M= Al–Cr, Cr, Zr) powders with different volume fractions of α-Fe, have been produced by HEBM and annealing. Optimum magnetic properties, namely the highest possible remanent magnetic polarization in association with an acceptable intrinsic coercivity, are obtained with a volume fraction of magnetically soft α-Fe phase of 37.5%, in agreement with theoretical predictions. The magnetic properties of a nanocrystalline two-phase $Nd_2(Fe,Co,M)_{14}B/\alpha$-Fe-type magnets can be tailored, to some extent, by the addition of additives that play a role in influencing the microstructure, such as grain size, crystallographic perfection and alignment of the constituent grains, and/or the intrinsic magnetic properties of the hard and soft phases. It has been found, in this work, that addition of small amount of Al–Cr, Cr, Zr to $Nd_2(Fe,Co,M)_{14}B/\alpha$-Fe improved the intrinsic coercivity and the hysteresis squareness of the $Nd_2(Fe,Co)_{14}B/\alpha$-Fe based nanocomposite materials. Partial replacement of Fe by Co in $Nd_2(Fe,Co)_{14}B/\alpha$-Fe increases the Curie temperature. These powders, with 37.5% by volume of α-Fe, would seem to offer most promise as bonded magnets, because they have an remanent magnetic polarizations of order of 1.1 T and an intrinsic coercivities of order of 700 kA m^{-1}.

Hot pressing of $Nd_2(Fe,Co,M)_{14}B/\alpha$-Fe with a 37.5% volume fraction of α-Fe produced a nanocomposite two-phase magnets with a remanent magnetic polarizations of 1.0 T, an intrinsic coercivities of 500 kA m^{-1} and a densities of 7.6 g cm^{-3}. The temperature coefficients of remanent magnetic polarization ($\alpha(J_r)$) and intrinsic coercivity ($\beta({}_JH_c)$) of nanocomposite $Nd_2(Fe,Co,M)_{14}B/\alpha$-Fe magnets in the temperature range of 293–413 K were studied and the results are compared with data for sintered Nd–Fe–B magnets. It is worth noting that partial replacement of Fe by Co, Zr or Al–Cr substantially reduces α and

β in $Nd_{12.6}Fe_{69.8}Co_{11.6}B_6$/α-Fe nanocomposite magnets with a 37.5% volume fraction of α-Fe. The temperature coefficients of remanence (α) and coercivity (β) of $Nd_{12.6}Fe_{69.3}Co_{11.6}Zr_{0.5}B_6$/α-Fe magnet, containing 37.5 vol% α-Fe, are -0.07 and $-0.35\%\ K^{-1}$, respectively. If the content of α-Fe phase in $Nd_2(Fe,Co,M)_{14}B$/α-Fe increases, the thermal stability of the intrinsic coercivity increases, too. The corrosion resistance is improved in the case of $Nd_{12.6}(Fe,Co,M)_{81.4}B_6$/α-Fe magnets ($M = Al_1Cr_2$) with a volume fraction of soft magnetic phase of 37.5 vol%. In the agglomerates, the α-Fe(Co) phase acts as a protective layer for the $Nd_2(Fe,Co,M)_{14}B$ nanograins against the oxidation.

Acknowledgements

One from the authors (JJ) is supported by a fellowship for young scientist from Foundation for Polish Science (2000).

References

[1] E.C. Stoner, E.P. Wohlfarth, Philos. Trans. R. Soc. A 240 (1948) 599.
[2] M. Jurczyk, S.J. Collocott, J.B. Dunlop, P.B. Gwan, J. Phys. D. Appl. Phys. 29 (1996) 2284.
[3] R.W. McCallum, A.M. Kadin, G.B. Clemente, J.E. Keem, J. Appl. Phys. 61 (1987) 3577.
[4] R. Coehoorn, D.B. de Mooij, J.P.W.B. Duchateau, K.H.J. Buschow, J. Phys. (Paris) C8 (1988) 669.
[5] W. Gong, G.C. Hadjipanayis, R.F. Krause, J. Appl. Phys. 75 (1994) 6649.
[6] M. Jurczyk, J.S. Cook, S.J. Collocot, J. Alloys Comp. 217 (1995) 65.
[7] M. Jurczyk, J. Alloys Comp. 235 (1996) 232.
[8] D. Goll, M. Seeger, H. Kronmüller, J. Magn, Magn. Mater. 185 (1998) 49.
[9] J. Ding, P.G. McCormick, R. Street, J. Magn. Magn. Mater. 124 (1993) L1.
[10] S. Hirosawa, H. Kanekiyo, M. Uehara, J. Appl. Phys. 73 (1993) 6488.
[11] E.F. Kneller, R. Hawig, IEEE Trans. Magn. 27 (1991) 3588.
[12] R. Skomski, J. Appl. Phys. 76 (1994) 7059.
[13] T. Schrefl, J. Fidler, H. Kronmüller, Phys. Rev. B 49 (1994) 6100.
[14] T. Schrefl, R. Fischer, J. Fidler, H. Kronmüller, J. Appl. Phys. 76 (1994) 7053.
[15] R. Fisher, T. Schrefl, H. Kronmüller, J. Fiedler, J. Magn. Magn. Mater. 150 (1995) 329.
[16] A. Manaf, R.A. Buckley, H.A. Davies, J. Magn. Magn. Mater. 128 (1993) 302.
[17] A.M. Gabay, A.G. Popov, V.S. Gavico, Y.V. Belozerov, A.S. Yermolenko, N.N. Shchegoleva, J. Alloys Comp. 237 (1996) 101.
[18] J. Wecker, K. Schnitzke, H. Cerva, W. Grogger, Appl. Phys. Lett. 67 (1995) 563.
[19] W.F. Miao, J. Ding, P.G. McCormick, R. Street, J. Alloys Comp. 240 (1996) 200.
[20] K.H.J. Buschow, Rep. Prog. Phys. 54 (1991) 1123.
[21] J.F. Herbst, Rev. Mod. Phys. 63 (1991) 819.
[22] J. Fidler, L. Yang, in: Proc. 4th Int. Symp. on Magnetic Anisotropy and Coercivity in Rare Earth–Transition Metal Alloys, Dayton, OH, 1985, p. 647.
[23] E. Adler, W. Rodewald, B. Wall, J. Appl. Phys. 70 (1991) 6637.
[24] P. Tenaud, H. Lemaire, F. Vial, in: EMMA '91, Dresden, Germany, 1991.
[25] J. Fidler, IEEE Trans. Magn. 21 (1985) 1955.
[26] F.E. Camp, A.S. Kim, J. Appl. Phys. 70 (1991) 6348.
[27] H. Nakamura, A. Fukuno, T. Yoneyama, in: Proc. 10th Int. Workshop on Rare Earth Magnets and their Applications, Kyoto, Japan, 1990, p. 341.
[28] S. Szymura, H. Bala, G. Pawłowska, Rabinovich, V.V. Sergeev, D.K. Pokrovskii, J. Less-Common Metals 175 (1991) 185.
[29] J. Fidler, in: Proc. 7th Int. Symp. on Magnetic Anisotropy and Coercivity in Rare Earth Transition Metal Alloys, Canberra, Australia, 1992, p. 11.
[30] J.M. Le Breton, J. Teillet, Hyperfine Interactions 94 (1994) 1909.
[31] H. Bala, G. Pawłowska, S. Szymura, V.V. Sergeev, Rabinovich, J. Magn. Magn. Mater. 87 (1990) 1255.
[32] H. Bala, S. Szymura, Inżynieria Materiałowa 3–4 (1995) 119.
[33] B.D. Cullity, Elements of X-ray Diffraction, Addison-Wesley, Reading, MA, 1978.
[34] M. Jurczyk, IEEE Trans. Magn. 24 (1988) 1942.
[35] M. Jurczyk, J. Magn. Magn. Mater. 73 (1988) 367.
[36] S. Hirosawa, H. Kanekiyo, Mater. Sci. Eng. A 217–218 (1996) 367.
[37] S. Hirosawa, H. Kanekiyo, in: Proc. 13th Int. Workshop on Rare Earth Magnets and their Applications, Birmingham, 1994, p. 87.
[38] J.M. Le Breton, S. Steyaert, M. Jurczyk, J. Teillet, in: Proc. 15th Int. Workshop on Rare-Earth Magnets and their Applications, Dresden, 1998, p. 887.
[39] J.M. Le Breton, S. Steyaert, J. Jakubowicz, M. Jurczyk, J. Teillet, to be published.
[40] Vacuumschmelze product catalogue (1998).